Hydrodeoxygenation of Phenolic Compounds by Sulfided (Co)Mo/Al2O3 Catalysts, a Combined Experimental and Theoretical Study

M. Badawi, J.F. Paul, E. Payen, Y. Romero, F. Richard, S. Brunet, A. Popov, E. Kondratieva, J.P. Gilson, L. Mariey, et al.

Dossier

This paper is a part of the hereunder thematic dossier published in OGST Journal, Vol. 68, No. 5, pp. 789-946 and available online here

Cet article fait partie du dossier thématique ci-dessous publié dans la revue OGST, Vol. 68, n°5, pp. 789-946 et téléchargeable ici

DOSSIER Edited by/Sous la direction de : **A. Daudin et A. Quignard**

PART 2

Second and Third Generation Biofuels: Towards Sustainability and Competitiveness

Deuxième et troisième génération de biocarburants : développement durable et compétitivité

Oil & Gas Science and Technology – Rev. IFP Energies nouvelles, Vol. 68 (2013), No. 5, pp. 789-946

789 > Editorial

801 > *Biomass Fast Pyrolysis Reactors: A Review of a Few Scientific Challenges and of Related Recommended Research Topics*
Réacteur de pyrolyse rapide de la biomasse : une revue de quelques verrous scientifi ques et d'actions de recherches recommandées
J. Lédé

815 > *Membrane Fractionation of Biomass Fast Pyrolysis Oil and Impact of its Presence on a Petroleum Gas Oil Hydrotreatment*
Fractionnement membranaire d'une huile de pyrolyse flash et impact de sa présence sur l'hydrotraitement d'un gazole atmosphérique
A. Pinheiro, D. Hudebine, N. Dupassieux, N. Charon and C. Geantet

829 > *Hydrodeoxygenation of Phenolic Compounds by Sulfided (Co)Mo/Al_2O_3 Catalysts, a Combined Experimental and Theoretical Study*
Hydrodésoxygénation de composés phénoliques en présence de catalyseurs sulfurés (Co)Mo/Al203 : une étude expérimentale et théorique
M. Badawi, J.-F. Paul, E. Payen, Y. Romero, F. Richard, S. Brunet, A. Popov, E. Kondratieva, J.-P. Gilson, L. Mariey, A. Travert and F. Maugé

841 > *Transformation of Sorbitol to Biofuels by Heterogeneous Catalysis: Chemical and Industrial Considerations*
Transformation du sorbitol en biocarburants par catalyse hétérogène : considérations chimiques et industrielles
L. Vilcocq, A. Cabiac, C. Especel, E. Guillon and D. Duprez

861 > *Biomass Conversion to Hydrocarbon Fuels Using the MixAlco™ Process*
Conversion de la biomasse en combustibles hydrocarbonés au moyen du procédé MixAlco™
S. Taco-Vasquez and M.T. Holtzapple

875 > *Algogroup: Towards a Shared Vision of the Possible Deployment of Algae to Biofuels*
Algogroup : vers une vision partagée du possible déploiement de la conversion des algues en carburants
X. Montagne, P. Porot, C. Aymard, C. Querleu, A. Bouter, D. Lorne, J.-P. Cadoret, I. Lombaert-Valot and O. Petillon

899 > *Towards a Microbial Production of Fatty Acids as Precursors of Biokerosene from Glucose and Xylose*
Vers une production microbienne d'acides gras en vue de l'application biokérosène à partir de glucose et xylose
M. Babau, J. Cescut, Y. Allouche, I. Lombaert-Valot, L. Fillaudeau, J.-L. Uribelarrea and C. Molina-Jouve

913 > *Insight on Biomass Supply and Feedstock Defi nition for Fischer-Tropsch Based BTL Processes*
Aperçu sur l'approvisionnement en biomasse et la caractérisation des charges pour les procédés de synthèse de biocarburants par voie BTL
J. Coignac

925 > *Second Generation Gazeous Biofuels: from Biomass to Gas Grid*
Biocarburants gazeux de 2e génération : du gisement de biomasse au réseau de gaz
O. Guerrini, M. Perrin and B. Marchand

935 > *BioTfueL Project: Targeting the Development of Second-Generation Biodiesel and Biojet Fuels*
Le projet BioTfueL : un projet de développement de biogazole et biokérosène de 2e génération
J.-C. Viguié, N. Ullrich, P. Porot, L. Bournay, M. Hecquet and J. Rousseau

Oil & Gas Science and Technology – Rev. IFP Energies nouvelles, No. 5, pp. 829-840

DOI: 10.2516/ogst/2012041

Dossier

Second and Third Generation Biofuels: Towards Sustainability and Competitiveness
Seconde et troisième génération de biocarburants : développement durable et compétitivité

Hydrodeoxygenation of Phenolic Compounds by Sulfided (Co)Mo/Al_2O_3 Catalysts, a Combined Experimental and Theoretical Study

M. Badawi[1,4], J.-F. Paul[1], E. Payen[1], Y. Romero[2], F. Richard[2*], S. Brunet[2], A. Popov[3], E. Kondratieva[3], J.-P. Gilson[3], L. Mariey[3], A. Travert[3*] and F. Maugé[3]

1 Unité de Catalyse et Chimie du Solide, Université Lille 1 Sciences et Technologies, CNRS, 59650 Villeneuve d'Ascq - France

2 Institut de Chimie des Milieux et Matériaux de Poitiers, UMR 7285, Université de Poitiers, CNRS, 4 rue Michel Brunet, BP 633, 86022 Poitiers Cedex - France

3 Laboratoire Catalyse et Spectrochimie, ENSICAEN, Université de Caen, CNRS, 6 Bd du Maréchal Juin, 14050 Caen - France

4 Laboratoire de Chimie et Physique des Milieux Complexes (LCPMC), Institut Jean Barriol FR2843 CNRS, Université de Lorraine, rue Victor Demange, 57500 Saint-Avold - France

e-mail: michael.badawi@univ-lorraine.fr - jean-francois.paul@univ-lille1.fr - edmond.payen@univ-lille1.fr - yilda.romero@univ-poitiers.fr frederic.richard@univ-poitiers.fr - sylvette.brunet@univ-poitiers.fr - andrei.popov@ensicaen.fr - elena.kondratieva@ensicaen.fr jean-pierre.gilson@ensicaen.fr - laurence.mariey@ensicaen.fr - arnaud.travert@ensicaen.fr - francoise.mauge@ensicaen.fr

* Corresponding author

Résumé — Hydrodésoxygénation de composés phénoliques en présence de catalyseurs sulfurés (Co)Mo/Al_2O_3 : une étude expérimentale et théorique — L'hydrodésoxygénation de deux composés phénoliques modèles (phénol et 2-éthylphénol)) a été étudiée sur deux catalyseurs Mo/Al_2O_3 et CoMo/Al_2O_3 sulfurés. La désoxygénation de ces molécules fait intervenir deux voies parallèles et indépendantes, à savoir :

– l'hydrogénation du noyau aromatique suivie par la rupture de la liaison C_{sp3}-O (voie HYD, (hydrogenation of the aromatic ring followed by Csp3-O bond cleavage)) ;
– la rupture directe de la liaison C_{sp2}-O (voie de DésOxygénation Directe – DOD).

Ces deux voies sont favorisées en présence du catalyseur promu par le cobalt (CoMo/Al_2O_3). La présence du groupe éthyle permet d'améliorer la voie DOD mais conduit à une diminution de la voie HYD. Les études menées par spectroscopie IR (InfraRouge) montrent que le phénol est majoritairement dissocié sur ces catalyseurs alors que le 2-éthylphénol semble plutôt adsorbé de façon non-dissociative. Les énergies d'adsorption de ces deux réactifs ainsi que celles des intermédiaires réactionnels impliqués sur les phases promues et non-promues ont été déterminées par calculs DFT *(Density-Functional Theory)*. Elles permettent de rationnaliser les résultats expérimentaux obtenus.

Abstract — Hydrodeoxygenation of Phenolic Compounds by Sulfided (Co)Mo/Al_2O_3 Catalysts, a Combined Experimental and Theoretical Study — *The hydrodeoxygenation of model phenol compounds (phenol and 2-ethylphenol) was carried over unpromoted Mo/Al_2O_3 and promoted CoMo/Al_2O_3 catalysts. Hydrodeoxygenation proceeds by two pathways:*

– *hydrogenation of the aromatic ring followed by C_{sp3}-O bond cleavage (HYD pathway*, (hydrogenation of the aromatic ring followed by Csp3-O bond cleavage)*);*
– *direct cleavage of the C_{sp2}-O bond (DDO pathway).*

Both routes were favored by the presence of Co on the catalyst, while the presence of the alkyl substituent on the phenolic ring favors the DDO route but inhibits the HYD pathway. IR (InfraRed) spectroscopy shows that while phenol mostly dissociates on these catalysts, a significant fraction of 2-ethylphenol remains non dissociated. The adsorption energies of both reactants and possible reaction intermediates on promoted and non-promoted sulfide phases as computed by DFT (Density-Functional Theory) confirm these findings and allow rationalizing the catalytic activity trends observed experimentally.

INTRODUCTION

The development of new biofuels is an attractive alternative to decrease both the consumption of fossil fuels and the emission of carbon dioxide. The European Union is committed to use non-food cellulosic and lignocellulosic biomass as a sustainable alternative of bio-fuel production [1]. Liquids derived from pyrolysis of lignocellulosic biomass [2-5] may be used without competing with a growing global demand for agricultural commodities but they contain large amounts of oxygenates (25-45 wt%) having multiple functions like aldehydes, ketones, acids, esters and alcohols [2-4]. They lead to deleterious properties such as high viscosity, thermal and chemical instability [3, 6] and poor engine efficiency. Hence, upgrading of bio-oils by reducing their oxygen content is required. Catalytic HydroDeOxygenation (HDO) to obtain oxygen-free molecules is one of processes that would allow to valorize these bio-oils.

Conventional sulfide catalysts used in hydrotreating processes such as (Co)Mo/Al_2O_3 appear as good candidates for HDO processing [2, 4, 6, 7]. The active phases of these catalysts consist of sulfide nano particles (MoS_2 or CoMoS) supported on high specific surface area alumina. These particles are made of MoS_2 sheets, the Co-promotor being localized on their (100) MoS_2 surface edges. The catalytic activity of these catalysts in hydrotreating reactions (HDS (hydrodesulfurization) or HDO) is usually related to the Coordinatively Unsaturated Sites (CUS sites) located on these edges, which accurate descriptions have been provided by a number of theoretical studies [8, 9].

A growing number of experimental studies deals with the HDO of lignocellulosic model compounds in model feeds [10-23] or in coprocessing with petroleum fractions [16, 17, 24, 25]. Phenolic compounds have been proved to be among the most refractory ones to the HDO process [2, 7]. Hydrodeoxygenation of these molecules proceeds by two pathways:

– hydrogenation of the aromatic ring followed by C_{sp^3}-O bond cleavage (HYD pathway);
– the direct cleavage of the C_{sp^2}-O bond (DDO pathway) [10-15, 17].

The Direct DeOxygenation (DDO) reaction pathway is desirable since it limits hydrogen consumption compared to the hydrogenation one.

The aim of the present work is to determine the nature of the catalytic active sites and the mechanisms involved during the hydrodeoxygenation of two model phenolic compounds (phenol and 2-ethylphenol) over conventional (Co)Mo/Al_2O_3 catalysts. To this aim, the reactivity of both compounds was evaluated at 613 K under 7 MPa, their interaction with the sulfide catalysts was monitored by IR spectroscopy and the reaction mechanisms were investigated using DFT modeling in order to rationalize experimental observations.

1 MATERIALS AND METHODS

1.1 Materials

The Mo/Al_2O_3 and CoMo/Al_2O_3 catalysts were prepared by conventional incipient wetness impregnation and supplied by *TOTAL*. Their chemical composition and textural properties are already reported in [14, 22] and summarized in Table 1. DiMethylDiSulfide (DMDS, 98%), phenol (99%), 2-ethylphenol (99%), toluene (99%) were purchased from *Aldrich*. CO (99.99%) was provided by *Air Liquide*.

TABLE 1

BET area, pore volume and chemical composition of the (Co)Mo/Al_2O_3 catalysts in their oxide form [14, 22]

	Mo/Al_2O_3	CoMo/Al_2O_3
BET area ($m^2.g^{-1}$)	251	255
Pore volume ($cm^3.g^{-1}$)	0.70	0.64
Mo (wt%)	9.9	9.2
Co (wt%)	-	4.2

1.2 Activity Measurements

The particle size of the catalysts was in the range of 250-315 µm. The catalysts were diluted in carborundum to keep the volume of the catalyst bed constant. In order to obtain comparable conversions (close to 20%), 50 mg of the Co-promoted catalyst or 100 mg of the unpromoted catalyst were used.

All the catalysts were sulfided *in situ* into a high-pressure dynamic flow reactor (length: 40 cm; inner diameter: 1.25 cm) using a mixture containing 5.8 wt% of DMDS diluted in toluene. Under 4.0 MPa of total pressure, the sulfiding mixture was injected at a starting temperature of 423 K. After 1 hour, the temperature was raised to 623 K at a rate of 5 $K.min^{-1}$ and it was maintained at this temperature for 14 hours. The temperature was then lowered to the reaction temperature (613 K).

The catalytic test was carried out under 7 MPa of total pressure using the oxygenated model compound (phenol or 2-ethylphenol), which was diluted in toluene. Their partial pressure was fixed to 49 kPa. DMDS was added to the feed to generate 30 kPa of H_2S in order to preserve the sulfide state and to prevent deactivation of the catalysts [15]. The partial pressure of hydrogen was kept constant at 5.75 MPa.

The reactor effluents were condensed and liquid samples were periodically analyzed with a *Varian* 3300 chromatograph equipped with a DB1 capillary column (length: 30 m; inside diameter: 0.50 mm; film thickness: 0.25 mm) and a flame ionization detector. The oven temperature was first set during 5 min at 328 K, then raised to 448 K at a rate of 4 $K.min^{-1}$ and kept at this temperature for 5 min.

Considering a differential reactor (total conversion near 20%), the deoxygenation activity (HDO) was calculated using the following equation:

$$A_{HDO} = X_{HDO}.F/W$$

where A_{HDO} is the deoxygenation activity (in mmol.h^{-1}.g^{-1}), X_{HDO} the conversion into deoxygenated products (in mol%), F the molar flow of the oxygenated reactant (in mmol.h^{-1}) and W the weight of sulfided catalyst (in g). The DDO, HYD and ACI (the ACI pathway involves the acidity of the catalyst) activities were calculated with the same formula. The conversion into deoxygenated products was replaced by the yield in aromatic products (benzene or ethylbenzene) for the determination of the DDO activity, by the yield in alkanes and alkenes compounds (ethylcyclohexane and ethylcyclohexenes for 2-ethylphenol, cyclohexane and cyclohexene for phenol) for the determination of the HYD activity and by the yield in oxygenated products for the determination of the ACI activity.

Both oxygenated reactants (phenol and 2-ethylphenol) were unreactive without catalyst. Over alumina alone, only 2-ethylphenol was transformed into oxygenates by isomerization, mainly leading to 3-ethylphenol and by disproportionation, yielding phenol and diethylphenol isomers, as already reported [14].

1.3 IR Spectroscopy

For the InfraRed (IR) study, the catalysts were grounded and pressed into self-supported wafers. After introduction in a low temperature IR cell, sulfidation was carried out *in situ* under a flow of H_2S/H_2 (10/90) at 623 K during 2 hours and followed by an evacuation during 1 hour at the same temperature.

Calibrated doses of phenol or 2-ethylphenol were introduced at Room Temperature (RT) up to a final equilibrium pressure of 20 Pa. Then, desorption was carried out at RT for 10 min evacuation prior to record the IR spectra.

The impact of phenol and 2-ethylphenol on the accessibility of the CUS sites of the sulfide phase was assessed using CO as a probe molecule. To this aim, CO was adsorbed on the freshly sulfided catalysts well as after phenol and 2-ethylphenol adsorption. After cooling at 100 K, calibrated doses of CO were introduced in the IR cell up to an equilibrium pressure of 133 Pa. For comparison, the spectra were normalized to 5 mg.cm^{-2} of the sulfided catalysts.

1.4 Computational Methods

The Density-Functional Theory (DFT, PW91 [26]) calculations were performed with the Vienna *Ab initio* Simulation Package (VASP) [27] using the PAW method [28]. The solution of the Kohn-Sham equations was improved self-consistently until a difference lower than 10^{-5} eV was obtained between successive iterations. The calculations were performed with a cut-off energy of 450 eV and a Methfessel-Paxton smearing with $\sigma = 0.1$ eV.

Throughout this work, we used a large super cell (12.641 × 12.294 × 25.000 Å^3), which contains four elementary MoS_2 units in the x and z direction and two layers along the y-axis *(Fig. 1)*. A k-point mesh (3,1,1) has been chosen to give an accurate sampling of the supercell's Brillouin zone.

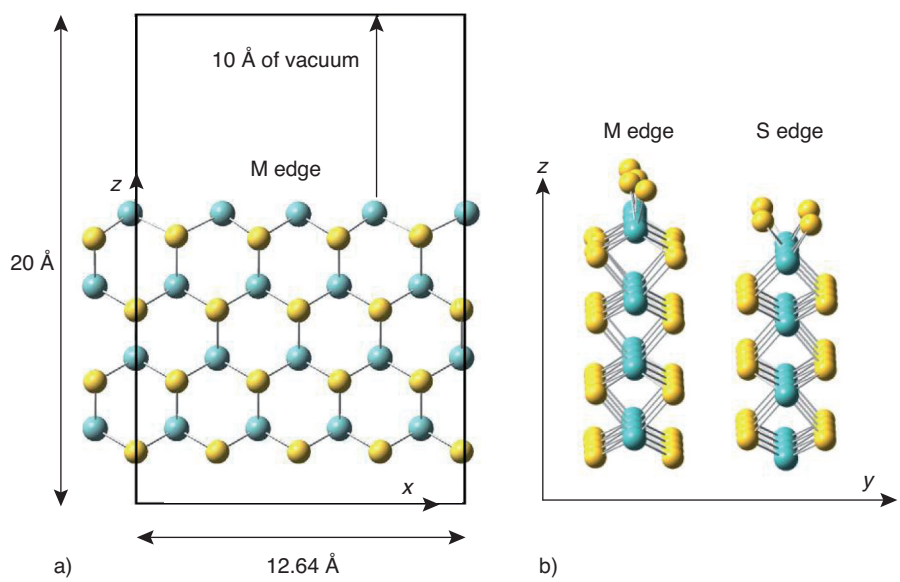

Figure 1

a) Cell showing the perfect MoS_2 (100) surface. b) Cell showing the stable MoS_2 surface when 0.05 < H_2S/H_2 < 10 000 [29] and H_2S/H_2O > 0.025 [29] that will be used as reference. Molybdenum atoms are in light blue, sulfur atoms are in yellow.

Previous studies [29-31] showed that this model is suitable to predict the electronic and structural properties of the MoS_2 surface. A vacuum layer of 15 Å is located above the MoS_2 slab in the *z* direction to avoid interactions between slabs. Since the molecules are adsorbed only on one side of the slab, dipolar corrections have been added in the *z* direction. The two upper rows were allowed to relax until forces acting on ions are smaller than 3.10^{-2} eV.Å^{-1}. The two lower rows were kept fixed to simulate bulk constraints [29-31]. The promoted catalyst is modeled by substituting of the Mo atoms on the S edge and half of the atoms on the metallic edge by Co *(Fig. 1)*, as proposed in literature [32]. The adsorption energy is computed following the next equation:

$$E_{ads} = E\,(\text{surface}) + E\,(\text{molecule}) - E\,(\text{molecule} + \text{surface})$$

Positive adsorption energy corresponds to an exothermic adsorption.

2 RESULTS AND DISCUSSION

2.1 Deoxygenation of Phenol and 2-ethylphenol over Mo/Al_2O_3 and $CoMo/Al_2O_3$

The transformation of phenol and 2-ethylphenol was carried out at 673 K under 7 MPa of total pressure over the unpromoted sulfide Mo/Al_2O_3 catalyst and the Co-promoted catalyst ($CoMo/Al_2O_3$). Over both catalysts, these oxygenated reactants are deoxygenated according to two pathways which are depicted in Figures 2 and 3. The first deoxygenation route involves a direct C-O bond scission (DDO pathway) yielding aromatic compounds: benzene from phenol and ethylbenzene from 2-ethylphenol. The second deoxygenation route, called the HYD pathway, leads probably, after hydrogenation of the aromatic ring, to an alcohol (cyclohexanol and 2-ethylcyclohexanol from phenol and 2-ethylphenol, respectively). These compounds are never detected, probably due to their easy dehydration into cycloalkenes. The dehydration of cyclohexanol yields only cyclohexene, whereas two isomers (1-ethylcyclohexene and 3-ethycyclohexene) are formed by the dehydration of 2-ethylcyclohexanol, the former is observed in higher quantities than the latter due to thermodynamics [14]. By hydrogenation, the corresponding alkane (cyclohexane or ethylcyclohexane) appears as the main product of the HYD pathway at conversion measured (close to 20%), whatever the sulfide catalyst used.

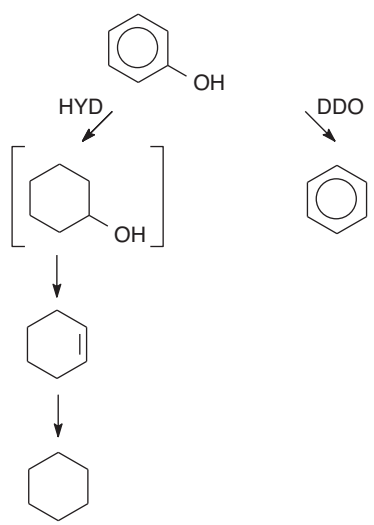

Figure 2

Reaction network for the deoxygenation of phenol over sulfide catalyst.

In the case of 2-ethylphenol, in addition to the two deoxygenation routes, a third pathway, called the ACI pathway (isomerization and disproportionation of ethylphenol), is also observed which mainly involves the acid properties of the catalyst support. This route leads to the formation of phenol, 3-ethylphenol and diethylphenol isomers. These products can also be deoxygenated, yielding benzene, cyclohexane, cyclohexene, diethylbenzenes and diethylcycloalkanes *(Fig. 3)*.

Table 2 reports the activity of both sulfide catalysts measured after 8 hours on stream. These results clearly indicate an inhibiting effect of the presence of the alkyl group in ortho position on the reactivity of the phenolic compound. Indeed, over both catalysts, phenol is 1.3 times more reactive in deoxygenation than 2-ethylphenol. These results are in accordance with those reported by Massoth *et al.* [12], which show that phenol was 1.5 times more reactive than 2-methylphenol over a $CoMo/Al_2O_3$ catalyst.

In addition, our results show that the difference of reactivity of these phenolic compounds depends on the deoxygenation pathway over both catalysts. Indeed, while the ethyl group in ortho position improves the DDO reactivity, 2-ethylphenol being more reactive than phenol, it is detrimental for the

TABLE 2

Activity and DDO/HYD selectivity of Mo/Al_2O_3 and $CoMo/Al_2O_3$ sulfide catalysts measured after 8 hours on stream during the hydrodeoxygenation of phenol and 2-ethylphenol at 613 K under 7 MPa of total pressure in presence of 30 kPa of H_2S in the feed. Promoting effect of Co (defined as the ratio between the activity of the promoted and the unpromoted catalyst) is given in brackets

Sulfided catalyst	Reactant	Activity (mmol.h^{-1}.g^{-1})				DDO/HYD selectivity
		HDO	DDO	HYD	ACI	
Mo/Al_2O_3	Phenol	10.3	1.0	9.3	-	0.11
	2-ethylphenol	7.6	1.6	5.3	4.4	0.30
$CoMo/Al_2O_3$	Phenol	29.1 (2.8)	7.4 (7.4)	21.7 (2.3)	-	0.34
	2-ethylphenol	22.0 (2.9)	10.4 (6.5)	10.0 (1.9)	5.7 (1.3)	1.04

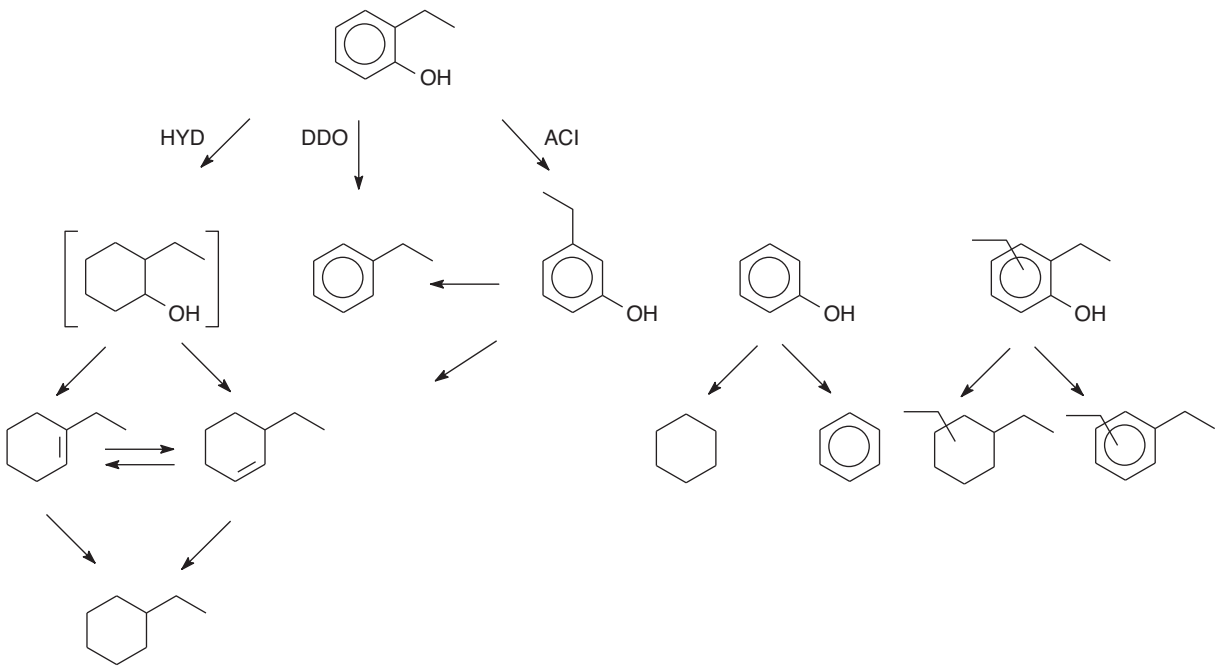

Figure 3

Reaction network for the transformation of 2-ethylphenol over sulfide catalyst.

HYD pathway since 2-ethylphenol is about twice less reactive than phenol. This latter result is in agreement with the results reported by Aubert *et al*. [33] over a $NiMo/Al_2O_3$ catalyst. As a consequence, the DDO/HYD selectivity is much higher for 2-ethylphenol deoxygenation (~1) than for phenol deoxygenation (~0.34) over $CoMo/Al_2O_3$ *(Tab. 2)*.

Moreover, Table 2 indicates a promoting effect of cobalt on deoxygenation of both phenolic compounds, since the Co-promoted catalyst is about 2.9 more active in deoxygenation than the unpromoted Mo/Al_2O_3 catalyst. Such a promoting effect was already reported in literature [14, 15] and was attributed to a decrease of the metal-sulfur bond allowing an easier formation of sulfur vacancies (CUS), which are proposed as active sites for such a reaction [14, 15, 21-23], while maintaining an optimal metal-heteroatom bond energy [34]. Moreover, we can underline that the effect of Co depends on the involved deoxygenation route: the DDO pathway is promoted in a larger extent than the HYD pathway, whatever the phenolic reactant. It is worth noticing that the reactivity of analogous sulfur containing compound significantly differs from that of phenolic compounds. In particular, thiophenol only reacts through the DDS pathway [35], preventing any comparison of the influence of the Co promotor on DDS(O)/HYD selectivities to be made. The differences on the reactivity of the two phenolic compounds investigated and on the Co promoting effect between the two deoxygenation pathways can be explained by several factors:

– the involvement of different active sites in the two deoxygenation pathways [22, 33];
– differences in the adsorption mode of the phenolic compounds (*e.g.* η_1 *vs* η_5 adsorption [14, 15, 23], dissociative *vs* non dissociative adsorption).

In order to get more insight in these phenomena, the adsorption of the phenolic compounds with both catalysts was studied by IR spectroscopy.

2.2 Infrared Characterization of Phenol and 2-ethylphenol Adsorption

Figure 4 shows the IR spectra of phenol and 2-ethylphenol in CCl_4 (spectra 1a and 2a, respectively) and the IR spectra obtained after adsorption on Al_2O_3 (spectra 1b and 2b) and $CoMo/Al_2O_3$ (spectra 1c and 2c). The spectra obtained on Mo/Al_2O_3 were similar to the latter and are not reported here. The assignment of the main IR bands of the phenolic compounds in solution, based on previous works [36, 37] are reported in Table 3.

The spectra obtained after phenol adsorption on Al_2O_3 (1b) and on $CoMo/Al_2O_3$ (1c) are qualitatively similar. They evidence the formation of phenate species characterized by bands at 1 597 cm^{-1}, 1 498-1 492 cm^{-1} (νCC_{ring}) and 1 295-1 271 cm^{-1} ($\nu CC_{ring} + \nu CO$). These bands have identical positions and relative intensities on Al_2O_3 and $CoMo/Al_2O_3$

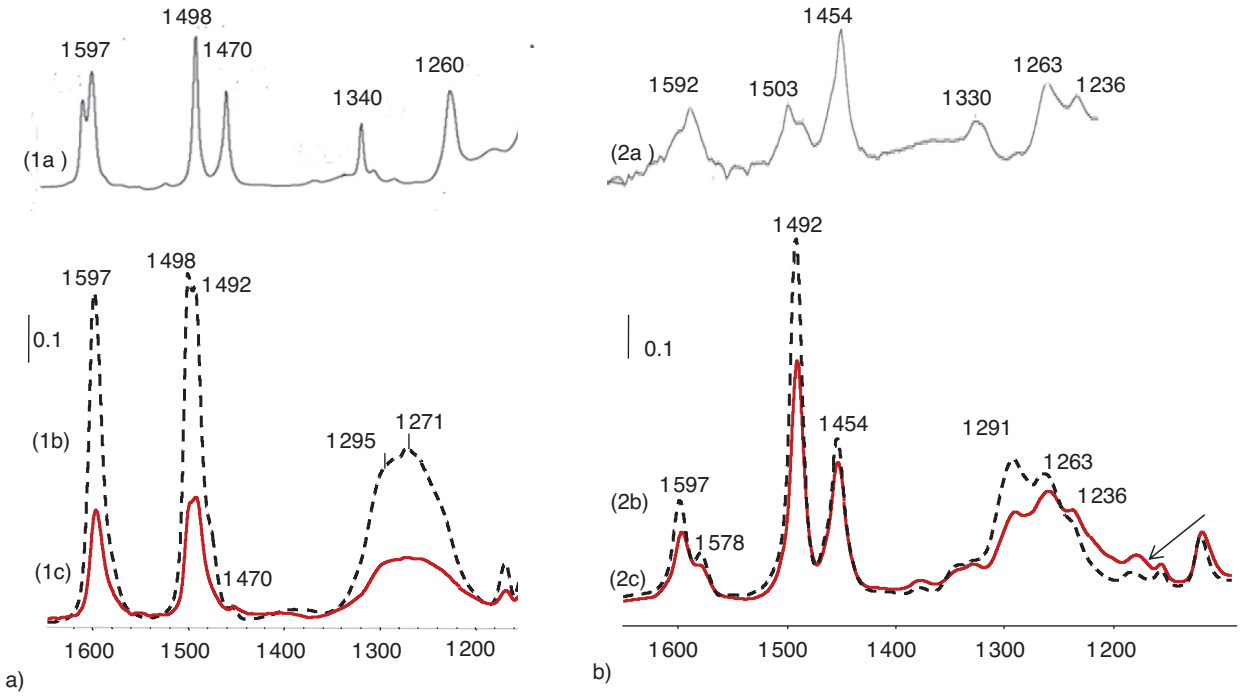

Figure 4

a) IR spectra of phenol in CCl_4 (1a), adsorbed on Al_2O_3 (1b dotted line) and on $CoMo/Al_2O_3$ (1c full line); b) IR spectra of 2-ethylphenol in CCl_4 (2a), adsorbed on Al_2O_3 (2b dotted line) and on $CoMo/Al_2O_3$ (2c full line).

TABLE 3

Assignment of IR bands of phenol and 2-ethylphenol in CCl_4

Assignment[a]	Phenol (in cm^{-1})	2-ethylphenol (in cm^{-1})
νCC_{ring}	1 600	1 592
νCC_{ring}	1 502	1 503
$\nu CC_{ring} + \delta OH$	1 473[a]	1 454
$\nu(CC_{ring}) + \delta OH$	1 340	1 330
$\nu CC_{ring} + \nu CO$	1 260	1 263, 1 236

[a] Assignment based on experiments with deuterated molecules.

but present much lower intensities on $CoMo/Al_2O_3$ indicating that phenol mostly dissociates on the support but does not interact strongly with the sulfide phase. The very weak intensity of the band at ~1 470 cm^{-1}, assigned to $\nu CC_{ring} + \delta OH$ vibrations of phenol *(Tab. 3)* indicates that in these conditions (adsorption followed by evacuation at room temperature), most of phenol species are dissociated on the Al_2O_3 support [38].

Spectra of 2-ethylphenol adsorbed on Al_2O_3 (2b) and $CoMo/Al_2O_3$ (2c) present bands at 1 597-1 578 cm^{-1} and 1 492 cm^{-1} (νCC_{ring}), 1 454 cm^{-1} ($\delta CH + \delta OH$) and 1 291, 1 263, 1 236 cm^{-1} ($\nu CC_{ring} + \nu CO$). In contrast with phenol adsorption, the large intensity of the band at 1 454 cm^{-1} indicates that a significant fraction of 2-ethylphenol is molecularly adsorbed on both surfaces. Moreover, the increase in the intensity ratio between this band and the νCC_{ring} band at 1 492 cm^{-1} on $CoMo/Al_2O_3$ provides evidence for a higher fraction of molecularly adsorbed 2-ethylphenol on $CoMo/Al_2O_3$ than on the pure Al_2O_3 support. As a supplementary indication of this observation, one can note the increased intensity ratio between ν(CO) bands at 1 263 cm^{-1}, 1 236 cm^{-1} (molecularly adsorbed form) and 1 291 cm^{-1} (2-ethylphenate) on $CoMo/Al_2O_3$.

Figure 5 shows the IR spectrum of CO adsorbed on the freshly sulfided $CoMo/Al_2O_3$ catalyst (spectrum a). It leads to the appearance of bands at 2 186 and 2 154 cm^{-1} corresponding to CO interacting with Lewis acid sites (Al^{3+}) and acidic AlO-H groups of the uncovered alumina support, a band at 2 110 cm^{-1} characterizing non promoted CUS Mo edge sites [39] and two bands at 2 070 and 2 052 cm^{-1} corresponding to promoted CUS sites in various environments [40].

CO adsorption on $CoMo/Al_2O_3$ after phenol adsorption (*Fig. 5*, spectrum b) shows the complete disappearance of the band at 2 186 cm^{-1} (Al^{3+} sites) and a large decrease of the band at 2 154 cm^{-1} (AlO-H hydroxyl groups). The νCO bands characterizing the sulfide phase are also markedly diminished, by nearly 60%. Similar but amplified effects are observed

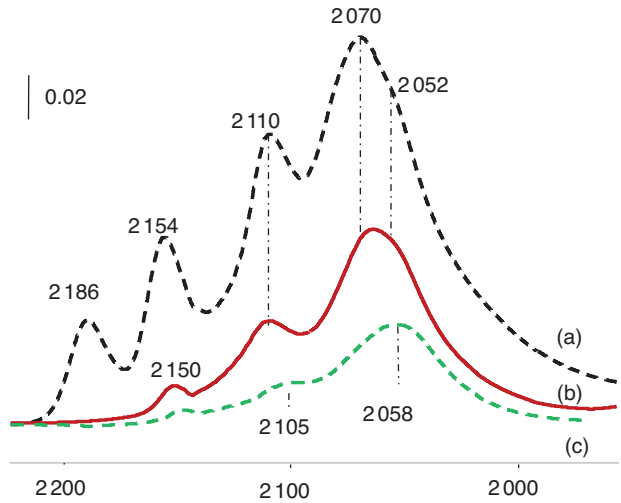

Figure 5

IR spectra of CO adsorbed on CoMo/Al_2O_3 after:
a) sulfidation; b) phenol adsorption at room temperature;
c) 2-ethylphenol adsorption at room temperature.

after 2-ethylphenol adsorption (*Fig. 5*, spectrum c) with a decrease of the intensity of the bands characterizing the sulfide phase of about 80% with a downward shift to 2 105 and 2 058 cm^{-1} which is not observed on the case of phenol adsorption (*Fig. 5*, spectrum b). This slight shift specifically observed in the case of 2 ethyl phenol could result from lateral interactions between CO and 2-ethylphenol adsorbed on the sulfide phase.

IR analysis of phenol and 2-ethylphenol adsorption on CoMo/Al_2O_3 thus shows that while phenol mostly adsorbs dissociatively, a significant fraction of 2-ethylphenol adsorbs molecularly on the Al_2O_3 support. The higher fraction of non-dissociated 2-ethylphenol observed on the CoMo/Al_2O_3 catalyst *vs* pure Al_2O_3 also suggests a non-dissociative adsorption on the sulfide phase in our conditions. This difference in adsorption modes is in line with the lower acidity of 2-ethylphenol (pKa = 10.20) as compared to phenol (pKa = 9.95), explaining why the former dissociates in a lower extent. While this infrared study does not provide direct evidence for phenol adsorption on the sulfide phase in our conditions, one may suggest that phenol adsorption on the sulfide phase, if any, is also dissociative.

This study also shows a decrease in the accessibility of the sulfide phase: both bands characteristic of CO adsorption on unpromoted and promoted sulfide sites decrease, which can be explained by direct or indirect blockage of these sites. In the case of phenol, the analysis of the spectra *(Fig. 4)* shows the absence of molecularly adsorbed phenol, indicating that the decrease of the unpromoted and promoted sites of the sulfide phase *(Fig. 5)* might result from the dissociative adsorption of phenol on these sites. The larger decrease of the amount of remaining CUS sites detected by CO after adsorption of 2-ethylphenol *(Fig. 5)* parallels the increase in the fraction of molecularly adsorbed species *(Fig. 4)*, suggesting that a part of this decrease is due to molecular adsorption of 2-ethylphenol on the CUS sites of the sulfide phase.

Finally, the decrease of the amount of CUS sites after adsorption of both phenolic compounds might also result from the presence of vicinal phenolate species on the support which might prevent the access of CO to the sulfide phase sites [38].

In order to get more insight on the adsorption behavior and reaction mechanisms of both phenolic compounds on the sulfide phase, DFT calculations have been carried out on non-promoted and promoted model surfaces.

2.3 DFT Modeling

DFT calculations were carried out on the metallic edges of non promoted MoS_2 and promoted CoMoS surfaces (50% Co substitution). Under HDO conditions, the presence of H_2, H_2S and H_2O will modify the stoechiometry and the nature of the atoms on the edges of the catalyst active phase. For the reaction conditions used in the experimental studies, the most MoS_2 stable surface [21] is presented in Figure 1. This figure shows that the molybdenum edge is covered with sulfur atoms, yielding sixfold-coordinated Mo edge atoms [29, 41]. Adsorption of large molecules will not be possible on this stable surface. The removal of one sulfur atom from the edge will lead to the formation of the active site. For the unpromoted catalyst, this departure is endothermic and the number of vacancy will be low. For the promoted catalyst, formally, one Mo-S group is substituted by one Co atom, creating stable vacancies on the edge. In this study, we consider a 50% substituted particle edge with two vacancies and two Mo=S groups per unit cell *(Fig. 6)* [32]. The reaction pathway of both molecules on these surfaces has been calculated for both DDO and HYD mechanisms.

2.3.1 Adsorption on Non-Promoted and Promoted Surfaces

Both non-dissociative and dissociative η_1 adsortptions of phenol and 2-ethylphenol were considered. The adsorption energies on the unpromoted phase are reported in Table 4, showing that the values for the non dissociative adsorption are similar for both molecules. The adsorption energies are slightly larger for 2-ethylphenol due to the inductive effect of the ethyl group. This increase demonstrates that the steric constraints are very small for an η_1 adsorption mode. The dissociation of the O-H group is possible on the unpromoted catalyst but the reaction is endothermic (17 $kJ.mol^{-1}$ for phenol and 48 $kJ.mol^{-1}$ for 2-ethylphenol). According to these values, equilibrium will be possible on the surface. The dissociation

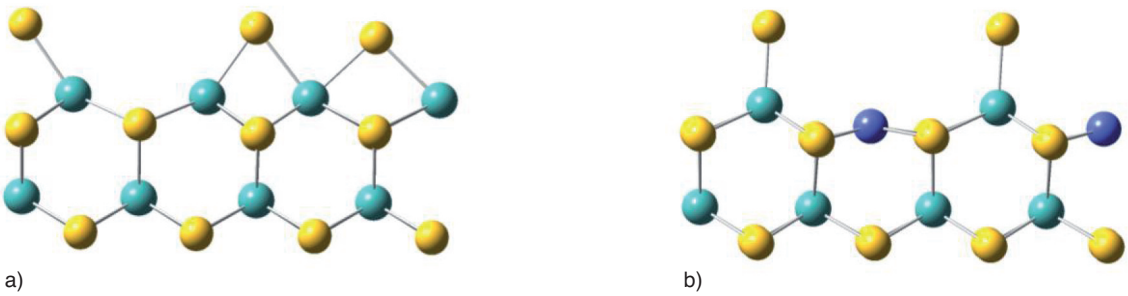

Figure 6

Representation of DDO adsorption sites over MoS_2 and CoMoS catalysts: a) vacancy on the MoS_2 M-edge; b) stable 50%-promoted CoMoS M-edge. Color code: Mo in light blue, S in yellow, Co in dark blue.

TABLE 4

Phenol and 2-ethylphenol η_1 adsorption energies (kJ.mol^{-1}) on the metallic edge of the unpromoted and promoted catalysts

	Adsorption mode	Phenol	2-ethylphenol
MoS_2	Non dissociative	28 *(Fig. 7a)*	39 *(Fig. 7b)*
	Dissociative	10	–9
CoMoS	Non dissociate	37	42 *(Fig 7e)*
	Dissociate	–55	–40

will be larger for the phenol in agreement with the pKa of both compounds and with the IR data reported above.

DFT calculations show that the adsorption by the aromatic ring is also possible on the metallic edge with one vacancy. However, due to the steric constraint the adsorption energy are negative for both η_2 (E_{ads} = –110 kJ.mol^{-1}; *Fig. 5c*) and η_6 (E_{ads} = –70 kJ.mol^{-1}; *Fig. 7d*) phenol adsorption modes. These values show that such adsorption modes are unlikely and this suggests that η_1 adsorption will be involved in both DDO and HYD mechanisms on these edges.

In the case of promoted surfaces, we have considered the 50% promoted M-edge *(Fig. 7)* that exhibits stable CUS sites under typical hydrotreating conditions [39]. The η_1 adsorption energies are similar to the ones observed for the unpromoted catalyst. They are slightly greater on the CoMoS promoted edge (E_{ads} = 37 kJ.mol^{-1} for phenol and E_{ads} = 42 kJ.mol^{-1} for 2-ethylphenol), and the difference between both molecules is smaller than over the unpromoted system. Table 4 also shows that the dissociative adsorption is more difficult on the promoted catalyst but the M=S group is less basic than the Mo-S-Mo group. The η_6 adsorption mode is very unlikely on the CoMo catalyst since the adsorption energy is negative (E_{ads} = –310 kJ.mol^{-1}), the surface deformation due to steric repulsions being responsible for this very large negative value *(Fig. 7)*.

The adsorption energies of phenol and 2-ethylpenol are significantly smaller than those previously reported of CO adsorption on similar surfaces [21, 35, 42]. This might explain why only few phenolic compounds adsorbed on the sulfide phase have been evidenced by IR spectroscopy. This also explains the inhibiting effect of CO on the HDO of phenolic compounds [13].

2.3.2 Direct Deoxygenation Mechanism

As DDO of phenolic compounds requires the activation of the C-O bond, the first step of this mechanism is the η_1 adsorption on CUS sites through the oxygen atom of these molecules. Our calculations show that the most efficient activation of the C-O bond is obtained when theses reactants are molecularly adsorbed on the CUS sites. The dissociation of the O-H group increases the C-O bond strength, as demonstrated by the evolution of the distance *i.e.* 1.39 Å for phenate and 1.42 Å for phenol. The same trend is observed on the CoMo catalyst (1.32 and 1.39 Å for phenate and phenol species, respectively).

The following step is the dissociative adsorption of H_2 on the surface, the adsorption of which being endothermic whatever the adsorption mode *(Fig. 8)*. Indeed, the displacement of atomic hydrogen from one Mo atom to a S atom is an athermic process [41].

The rate determining step is the addition of the proton on the carbon atom bearing the OH group, leading to a Wheland complex. On the non-promoted surface, the activation energy required for this step is close to 95 kJ.mol^{-1} for 2-ethylphenol and 110 kJ.mol^{-1} for phenol. Such a difference can be explained by a better stabilization of the carbocation due to the inductive effect of the ethyl group in the case of 2-ethylphenol. The computed activation energies on the promoted catalyst are slightly reduced but rank similarly (90 kJ.mol^{-1} for 2-ethylphenol and 100 kJ.mol^{-1} for phenol). The effect of cobalt is slightly larger for phenol (–10 kJ.mol^{-1}) than for 2-ethylphenol (–5 kJ.mol^{-1}). Besides, these results are in line with the higher DDO reactivity of 2-ethylphenol observed experimentally on both catalysts *(Tab. 2)*.

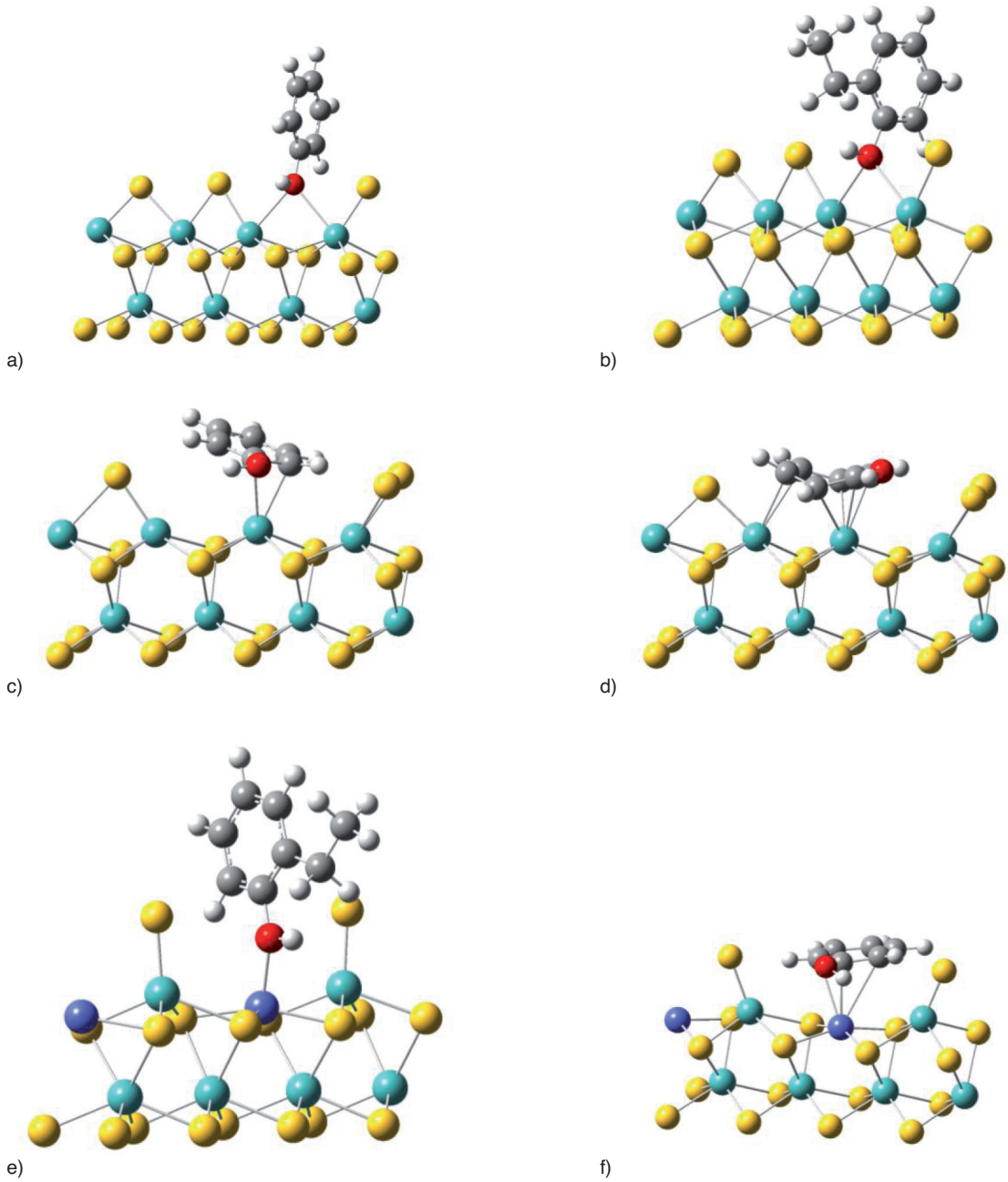

Figure 7

Representation of phenol and 2-ethylphenol adsorption modes on MoS_2 and CoMoS phases. a) η_1 adsorption mode of phenol on MoS_2; b) η_1 adsorption mode of 2-ethylphenol on MoS_2; c) η_2 adsorption mode of phenol on MoS_2; d) η_6 adsorption mode of phenol on MoS_2; e) η_1 adsorption mode of 2-ethylphenol on CoMoS; f) η_6 adsorption mode of phenol on CoMoS. Color code: Mo in light blue, S in yellow, Co in dark blue, C in grey, O in red, H in white.

Finally, C-O bond scission occurs, which leads to the formation of the aromatic product and an OH group adsorbed on the surface, the last step of the catalytic cycle being the departure of the water from the surface. This step is endothermic since the adsorption of water on the vacancy is exothermic [23]. However, because of the low concentration of water in the gas phase, the water desorption should be thermodynamically favored *(Fig. 8)* [21].

The present mechanism differs from the mechanism proposed by Dupond *et al.* [43] for the HDO of aliphatic alcohols. In the later case, the rate determining step is a C-O/C-S bond exchange leading to the formation of a thiol.

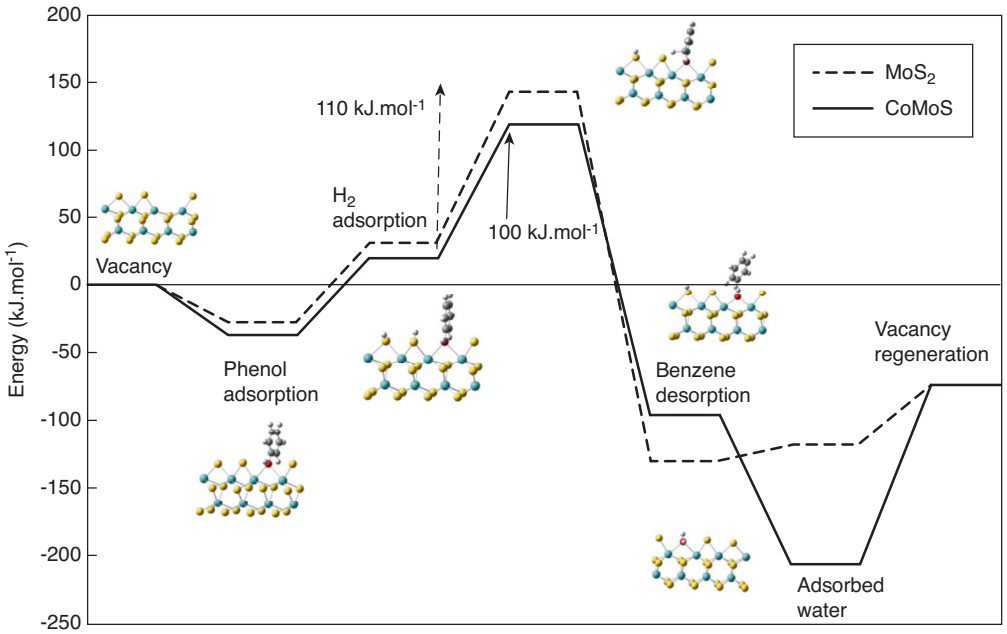

Figure 8

Reaction pathway for phenol DDO on MoS_2 and CoMoS sulfide phases. Color code: Mo in light blue, S in yellow, Co in dark blue, C in grey, O in red, H in white.

However, the same exchange is unlikely for phenol molecules, for which the C-O bond is strengthened by the electron delocalization. The activation energy will thus be much larger than either the activation energy computed for aliphatic alcohol (143 kJ.mol^{-1} [43]) and or than the activation energy calculated for the phenyl ring protonation (110 kJ.mol^{-1}, *Fig. 8*).

2.3.3 Hydrogenation (HYD) Mechanism

As no η_6 adsorption is possible on the sulfur edge, a hydrogenation mechanism involving an η_1 adsorption through the oxygen atom is considered in the present work. In such a configuration, the first hydrogen addition should occur on the carbon atoms in β position with respect to the oxygen atom, because:

- addition on the carbon in α position would result in the direct CO bond cleavage (DDO pathway);
- the other carbon atoms are located at distances too large from the surface for such an attack.

In this case, the first hydrogen addition consists in a proton attack from a sulfhydryl group in the vicinity of the β carbon atom of the aromatic ring *(Fig. 9)*. Although a hydride addition cannot be completely ruled out, such a situation is less likely because of the larger distance between hydrides bonded to a metallic atom and the β carbon. This attack in β position results in the formation of a Wheland complex which energy was found to be higher for an attack on the tertiary carbon atom bearing the ethyl group of 2-ethylphenol *(Fig. 9b)* than on the secondary carbon atoms of either phenol or 2-ethylphenol *(Fig. 9a)*. The difference between these two reaction energies is about 25 kJ.mol^{-1}. Hence, phenol should be statistically almost twice more reactive than 2-ethylphenol. This result is in very good agreement with our experimental results showing that the HYD reactivity of 2-ethylphenol is about twice lower than that of phenol *(Tab. 2)*.

Finally, our calculations also show that the formation of the Wheland complex involved on the HYD route is always favoured (by more than 30 kJ.mol^{-1}) when phenolic compounds are dissociatively adsorbed on the surface. This leads to an increased negative charge on the carbon atoms in β position, which favors the protonation of the aromatic ring as compared to the non-dissociative adsorption. As shown by both IR characterization *(Fig. 5)* and DFT calculations, the dissociative adsorption of phenol is favoured as compared to that of 2-ethylphenol, which also explains the higher HYD reactivity of phenol over both catalysts *(Tab. 2)*.

CONCLUSIONS

The main findings of the present study may be summarized as follows:

- 2-ethylphenol is more reactive than phenol in the DDO pathway which involves the direct cleavage of the C-O bond but less reactive in the HYD pathway involving prior hydrogenation of the aromatic ring;
- Co promotes both pathways in different extents, the DDO pathway being much more promoted that the HYD pathway;

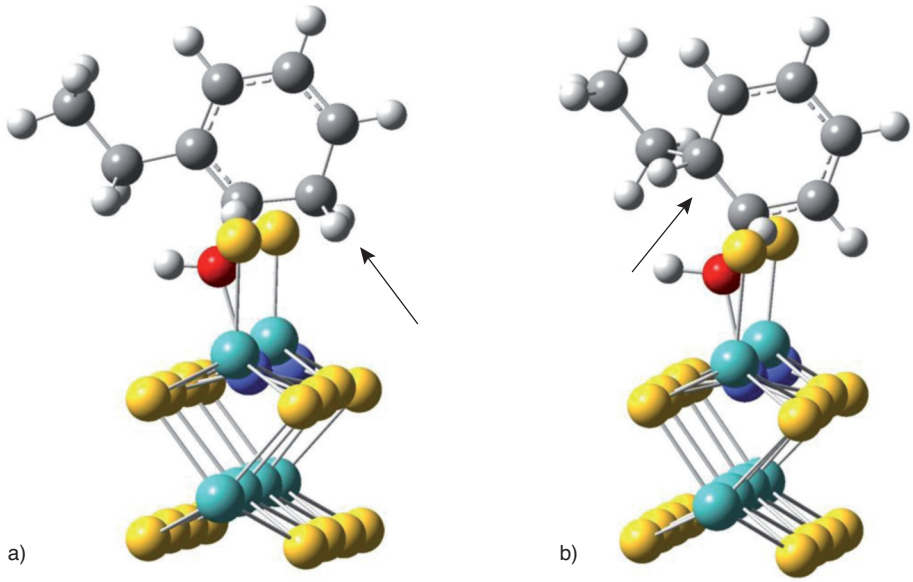

Figure 9

Representation of the Wheland intermediate formed in the hydrogenation pathway on CoMo. a) Addition on the secondary carbon; b) addition on the tertiary carbon. Color code: Mo in light blue, S in yellow, Co in dark blue, C in grey, O in red, H in white.

– IR spectroscopy shows that while phenol easily dissociates on these catalysts, adsorption of 2-ethylphenol leads to a larger amount of molecularly adsorbed species;
– DFT calculations show that both pathways can occur on CUS sites, after η_1 adsorption and protonation on either the carbon atom bearing the OH group (DDO pathway) or the carbon atoms on β position with respect to the oxygen atom (HYD pathway), which allows us to explain our main experimental findings.

ACKNOWLEDGMENTS

This work has been performed within the ANR funded Programme National de Recherche sur les Bioénergies EcoHdoc, a joint project of the Centre National de la Recherche Scientifique (CNRS), the Universities of Caen, Lille and Poitiers, and TOTAL and the Programme Interdisciplinaire Energie of CNRS. We acknowledge the USTL Centre de Ressources Informatiques (partially funded by FEDER) for allocating CPU time.

REFERENCES

1 Directive 2009/30/EC of the European Parliament and of the Council of 23 April 2009, amending Directive 98/70/EC as regards the specification of petrol, Diesel and gas-oil and introducing a mechanism to monitor and reduce greenhouse gas emissions and amending Council Directive 1999/32/EC as regards the specification of fuel used by inland waterway vessels and repealing Directive 93/12/EEC.

2 Furimsky E. (2000) Catalytic hydrodeoxygenation, *Appl. Catal. A: Gen.* **199**, 147-190.

3 Huber G.W., Corma A. (2007) Synergies between Bio- and Oil Refineries for the Production of Fuels from Biomass, *Ang. Chem. Int. Ed.* **46**, 7184-7201.

4 Huber G.W., Iborra S., Corma A. (2006) Synthesis of transportation fuels from biomass: chemistry, catalysts and engineering, *Chem. Rev.* **106**, 4044-4098.

5 Elliott D.C. (2007) Historical Developments in Hydroprocessing Bio-oils, *Energy Fuels* **21**, 1792-1815.

6 Czernik S., Bridgwater A.V. (2004) Overview of Applications of Biomass Fast Pyrolysis Oil, *Energy Fuels* **18**, 590-598.

7 Mortensen P.M., Grunwaldt J.-D., Jensen P.A., Knudsen K.G., Jensen A.D. (2011) A review of catalytic upgrading of bio-oil to engine fuels, *Appl. Catal. A: Gen.* **407**, 1-19.

8 Raybaud P. (2007) Understanding and predicting improved sulfide catalysts: Insights from first principles modeling, *Appl. Catal. A: Gen.* **322**, 76-91.

9 Paul J.-F., Cristol S., Payen E. (2008) Computational studies of (mixed) sulfide hydrotreating catalysts, *Catal. Today* **130**, 139-148.

10 Viljava T.-R., Komulainen R.S., Krause A.O.I. (2000) Effect of H_2S on the stability of $CoMo/Al_2O_3$ catalysts during hydrodeoxygenation, *Catal. Today* **60**, 83-92.

11 Senol O.I., Ryymin E.-M., Viljava T.-R., Krause A.O.I. (2007) Effect of hydrogen sulphide on the hydrodeoxygenation of aromatic and aliphatic oxygenates on sulphided catalysts, *J. Mol. Catal. A: Chemistry* **277**, 107-112.

12 Massoth F.E., Politzer P., Concha M.C., Murray J.S., Jakowski J., Simons J. (2006) Catalytic Hydrodeoxygenation of Methyl-Substituted Phenols: Correlations of Kinetic Parameters with Molecular Properties, *J. Phys. Chem. B* **110**, 14283-14291.

13 Romero Y., Richard F., Renème Y., Brunet S. (2009) Hydrodeoxygenation of benzofuran and its oxygenated derivatives (2,3-dihydrobenzofuran and 2-ethylphenol) over $NiMoP/Al_2O_3$ catalyst, *Appl. Catal. A: Gen.* **353**, 46-53.

14 Romero Y., Richard F., Brunet S. (2010) Hydrodeoxygenation of 2-ethylphenol as a model compound of bio-crude over sulfided Mo-based catalysts: Promoting effect and reaction mechanism, *Appl. Catal. B: Env.* **98**, 213-223.

15 Bouvier C., Romero Y., Richard F., Brunet S. (2011) Effect of H_2S and CO on the transformation of 2-ethylphenol as a model compound of bio-crude over sulfided Mo-based catalysts: Propositions of promoted active sites for deoxygenation pathways based on an experimental study, *Green Chem.* **13**, 2441-2451.

16 Pinheiro A., Hudebine D., Dupassieux N., Geantet C. (2009) Impact of Oxygenated Compounds from Lignocellulosic Biomass Pyrolysis Oils on Gas Oil Hydrotreatment, *Energy Fuels* **23**, 1007-1014.

17 Bui V.N., Toussaint G., Laurenti D., Mirodatos C., Geantet C. (2009) Co-processing of pyrolisis bio oils and gas oil for new generation of bio-fuels: Hydrodeoxygenation of guaïacol and SRGO mixed feed, *Catal. Today* **143**, 172-178.

18 Popov A., Kondratieva E., Goupil J.M., Mariey L., Bazin P., Gilson J.P., Travert A., Maugé F. (2010) Bio-oils Hydrodeoxygenation: Adsorption of Phenolic Molecules on Oxidic Catalyst Supports, *J. Phys. Chem. C* **114**, 15661-15670.

19 Bui V.N., Laurenti D., Afanasiev P., Geantet C. (2011) Hydrodeoxygenation of guaiacol with CoMo catalysts. Part I: Promoting effect of cobalt on HDO selectivity and activity, *Appl. Catal. B: Env.* **101**, 239-245.

20 Philippe M., Richard F., Hudebine D., Brunet S. (2010) Inhibiting effect of oxygenated model compounds on the HDS of dibenzothiophenes over $CoMoP/Al_2O_3$ catalyst, *Appl. Catal. A: Gen.* **383**, 14-23.

21 Badawi M., Cristol S., Paul J.-F., Payen E. (2009) DFT study of furan adsorption over stable molybdenum sulfide catalyst under HDO conditions, *C. R. Chim.* **12**, 754-761.

22 Badawi M., Paul J.-F., Cristol S., Payen E., Romero Y., Richard F., Brunet S., Lambert D., Portier X., Popov A., Kondratieva E., Goupil J.M., El Fallah J., Gilson J.-P., Mariey L., Travert A., Maugé F. (2011) Effect of water on the stability of Mo and CoMo hydrodeoxygenation catalysts: A combined experimental and DFT study, *J. Catal.* **282**, 155-164.

23 Badawi M., Paul J.-F., Cristol S., Payen E. (2011) Guaiacol derivatives and inhibiting species adsorption over MoS_2 and CoMoS catalysts under HDO conditions: A DFT study, *Catal. Commun.* **12**, 901-905.

24 Mercader F.M., Groeneveld M.J., Kersten S.R.A., Way N.W.J., Schaverien C.J., Hogendoorn J.A. (2010) Production of advanced biofuels: Co-processing of upgraded pyrolysis oil in standard refinery units, *Appl. Catal. B: Env.* **96**, 57-66.

25 Mercader F.M., Groeneveld M.J., Kersten S.R.A., Geantet C., Toussaint G., Way N.W.J., Schaverien C.J., Hogendoorn K.J.A. (2011) Hydrodeoxygenation of pyrolysis oil fractions: process understanding and quality assessment through co-processing in refinery units, *Energ. Environ. Sci.* **4**, 985-997.

26 Perdew J.P., Chevary J.A., Vosko S.H., Jackson K.A., Pedersen M.R., Singh D.J., Frolais C. (1992) Atoms, molecules, solids and surfaces: Applications of the generalized gradient approximation for exchange and correlation, *Phys. Rev. B* **46**, 6671-6687.

27 Kresse G., Hafner J. (1993) *Ab initio* molecular dynamics for liquid metals, *Phys. Rev. B* **47**, 558-561.

28 Kresse G., Joubert J. (1999) From ultrasoft pseudopotentials to the projector augmented-wave method, *Phys. Rev. B* **59**, 1758-1775.

29 Cristol S., Paul J.-F., Payen E., Bougeard D., Clemendot S., Hutschka F. (2000) Theoretical Study of the MoS_2 (100) Surface: A Chemical Potential Analysis of Sulfur and Hydrogen Coverage, *J. Phys. Chem. B* **104**, 47, 11220-11229S.

30 Cristol S., Paul J.-F., Schovsbo C., Veilly E., Payen E. (2006) DFT study of thiophene adsorption on molybdenum sulphide, *J. Catal.* **239**, 145-153.

31 Paul J.-F., Cristol S., Payen E. (2008) Computational studies of (mixed) sulfide hydrotreating catalysts, *Catal. Today* **130**, 139-148.

32 Krebs E., Silvi B., Raybaud P. (2008) Mixed sites and promoter segregation: A DFT study of the manifestation of Le Chatelier's principle for the Co(Ni)MoS active phase in reaction conditions, *Catal. Today* **130**, 160-169.

33 Aubert C., Durand R., Geneste P., Moreau C. (1988) Factors affecting the hydrogenation of substituted benzenes and phenols over a sulfided $Ni\text{-}O\text{-}MoO_3/\gamma\text{-}Al_2O_3$ catalyst, *J. Catal.* **112**, 12-20.

34 Toulhoat H., Raybaud P. (2003) Kinetic interpretation of catalytic activity patterns based on theoretical chemical descriptors, *J. Catal.* **216**, 63-72.

35 Viljava T.-R., Krause A.O.I. (1996) Hydrotreating of compounds containing both oxygen and sulfur: Effect of para-hydroxyl substituent on the reactions of mercapto and methylmercapto groups, *Appl. Catal. A: Gen.* **145**, 237-251.

36 Evans J.C. (1960) The vibrational spectra of phenol and phenol-OD, *Spectrochim. Acta* **16**, 1382-1392.

37 Roth W., Imhof P., Gerhards M., Schumm S., Kleinermanns K. (2000) Reassignment of ground and first excited state vibrations in phenol, *Chem. Phys.* **252**, 247-256.

38 Popov A., Kondratieva E., Gilson J.-P., Mariey L., Travert A., Maugé F. (2011) IR study of the interaction of phenol with oxides and sulfided CoMo catalysts for bio-fuel hydrodeoxygenation, *Catal. Today* **172**, 132-135.

39 Travert A., Dujardin C., Mauge F., Veilly E., Cristol S., Paul J.-F., Payen E. (2006) CO Adsorption on CoMo and NiMo Sulfide Catalysts: A Combined IR and DFT Study, *J. Phys. Chem. B* **110**, 1261-1270.

40 Travert A., Dujardin C., Maugé F., Cristol S., Paul J.-F., Payen E., Bougeard D. (2000) Parallel between infrared characterisation and *ab initio* calculations of CO adsorption on sulphided Mo catalysts, *Catal. Today* **70**, 255-269.

41 Travert A., Nakamura H., van Santen R.A., Cristol S., Paul J.-F., Payen E. (2002) Hydrogen Activation on Mo-Based Sulfide Catalysts, a Periodic DFT Study, *J. Am. Chem. Soc.* **124**, 24, 7084-7095.

42 Pelardy F., Dupont C., Fontaine C., Devers E., Daudin A., Bertoncini F., Raybaud P., Brunet S. (2010) Impact of CO on the transformation of a model FCC gasoline over $CoMoS/Al_2O_3$ catalysts: A combined kinetic and DFT approach, *Appl. Catal. B: Env.* **97**, 323-332.

43 Dupond C., Lemeur R., Daudin A., Raybaud P. (2011) Hydrodeoxygenation pathways catalyzed by MoS_2 and NiMoS active phases: A DFT study, *Catal.* **279**, 276-286.

Final manuscript received in July 2012
Published online in April 2013